Interface features and electronic structure of Bi2SiO5/β-Bi2O3 hetero-junction

Kovaleva, E., Vodyankina, O., Svetlichny, V.

E. A. Kovaleva, O. V. Vodyankina, V. A. Svetlichny, "Interface features and electronic structure of Bi2SiO5/β-Bi2O3 hetero-junction," Proc. SPIE 12086, XV International Conference on Pulsed Lasers and Laser Applications, 120860F (2 December 2021); doi: 10.1117/12.2614020

SPIE.

Event: XV International Conference on Pulsed Lasers and Laser Applications, 2021, Tomsk, Russian Federation

Interface features and electronic structure of Bi_2SiO_5/β-Bi_2O_3 hetero-junction

E.A. Kovaleva*, O.V. Vodyankina, V.A. Svetlichnyi
Laboratory of Catalytic Research, Tomsk State University, 36 Lenin Ave., Tomsk, Russia 634050

ABSTRACT

Atomic and electronic structure of Bi_2SiO_5/β-Bi_2O_3 hetero-junction was described by means of density functional theory. The interface was found to be narrow-gap semiconductor with indirect band gap. The redistribution of states near the Fermi level in hybrid structure and the impact of spin-orbit coupling are discussed.

Keywords: bismuth metasilicate, bismuth oxide, interface, heterostructure, density functional theory

1. INTRODUCTION

Renewable energy sources have gained research interest for decades. Solar energy catalysis is considered to be one of safe and sustainable alternatives to fossil fuel. There are a number of Bi-based materials with promising photocatalytic properties[1]. Though being promising photocatalysts, bismuth silicates are less investigated comparing to other bismuth compounds. Bismuth metasilicate Bi_2SiO_5 is of a particular research interest due to its perovskite-like structure and higher photocatalytic activity[2].

Computational chemistry is widely used to explain and predict the properties of materials. There are some papers devoted to Bi silicates utilizing both experimental techniques and DFT to shed the light on their optical behavior and electronic structure[3-8]. However, there's only a few papers[9] considering the interfacial structures while they tend to be crucial for our understanding of the catalyst formation. The present work is aimed to describe β-Bi_2O_3/Bi_2SiO_5 interface as the model for photocatalytically active Bi-based composites formation in terms of its atomic and electronic structure.

2. COMPUTATIONAL DETAILS

All calculations were performed within the framework of density functional theory. Geometry optimization of bulk β-Bi_2O_3 and Bi_2SiO_5 was carried out using GGA-PBE exchange-correlation functional[10,11], plane wave basis set and PAW method[12,13], as implemented in VASP[14-17]. Plane wave cutoff energy was equal to 400 eV. The Mönkhorst-Pack[18] scheme was implemented for k-point Brilloin zone sampling. k-mesh contained 3*3*6 points for β-Bi_2O_3 and 1*6*6 for Bi_2SiO_5 with respect to their unit cell sizes. Residual forces acting on atoms being less than 0.02 eV/Å were used as stopping criteria for geometry optimization. Then, in order to get correct values of the bandgap, single-point band structure calculations were carried out using hybrid functionals.

Slab and interface calculations were performed in OpenMX package which is known to be more efficient for these purposes as it uses pseudo-atomic orbitals instead of plane waves. Recommended basis sets and norm-conserving Vanderbilt pseudopotenials[19] were used. Grimme D3[20] correction was used to account for weak dispersion interactions. Vacuum interval of ~10 Å normal to the slab surface was used to eliminate the interaction of neighbor images. Surface slabs were fully relaxed until the forces acting on atoms were less than 0.01 ev/Å. One unit cell thick Bi_2SiO_5 and two unit cells thick β-Bi_2O_3 surfaces were modeled. 3*3*1 k-point mesh was used for both slabs and interface calculations.

3. RESULTS AND DISCUSSION

3.1 Bulk Bi_2SiO_5 and β-Bi_2O_3 structures

First, atomic and electronic structure of Bi_2SiO_5 bismuth metasilicate and β-Bi_2O_3 was studied. Unit cell parameters and comparison with available data are summarized in Table 1. Calculated cell vectors and angles are in good agreement with experimental ones.

*kovaleva.evgeniya1991@mail.ru

XV International Conference on Pulsed Lasers and Laser Applications, edited by Anton V. Klimkin, Maxim V. Trigub, Victor F. Tarasenko, Proc. of SPIE Vol. 12086, 120860F · © 2021 SPIE · 0277-786X · doi: 10.1117/12.2614020

Table 1. Unit cell parameters for β-Bi_2O_3 and Bi_2SiO_5.

Compound	VASP			OpenMX			Reference		
	a, Å	b, Å	c, Å	a, Å	b, Å	c, Å	a, Å	b, Å	c, Å
β-Bi_2O_3	7.74	7.74	5.57	7.83	7.83	5.65	7.74[21]	7.74[21]	5.64[21]
Bi_2SiO_5	15.12	5.48	5.29	15.25	5.56	5.34	15.17[22]	5.47[22]	5.31[22]

Figure 1 illustrates band structures calculated for β-Bi_2O_3 и Bi_2SiO_5 within GGA-PBE approximation. β-Bi_2O_3 is indirect semiconductor with E_g value of 1.31 eV. Bi_2SiO_5 shows wide direct band gap of 2.81 eV.

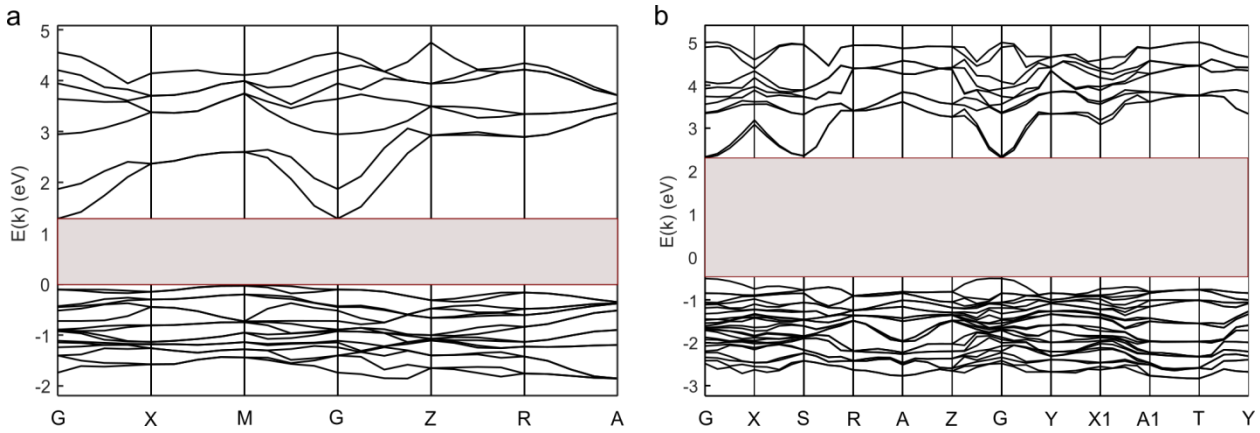

Figure 1. Band structures for β -Bi_2O_3 (a) and Bi_2SiO_5 (b). Band gap is defined by darker rectangle.

GGA exchange-correlation functionals are known to underestimate the band gap. Keeping that in mind, a series of extra hybrid functional calculations was performed using PBE0, B3LYP, HSE06 functionals. Densities of states (DOS) for β-Bi_2O_3 are presented in Figure 2. Only PBE0 functional is presented as a reference for hybrid ones as B3LYP and HSE06 demonstrate basically the same results with only conduction band bottom location different. Peak shape of PBE0 DOS is different from GGA-PBE ones due to the different smearing method applied. Tetrahedron method was used in standard GGA-PBE calculations while Gaussian smearing with σ=0.1 eV was used in hybrid calculations. Meeting our expectations, it does become wider when hybrid functional applied. PBE0 tend to demonstrate the largest E_g values while HSE06 ones are up to 0.7 eV lower. B3LYP results lie in between of those (see Table 2). All the mentioned features and trends are valid for Bi_2SiO_5 compound as well.

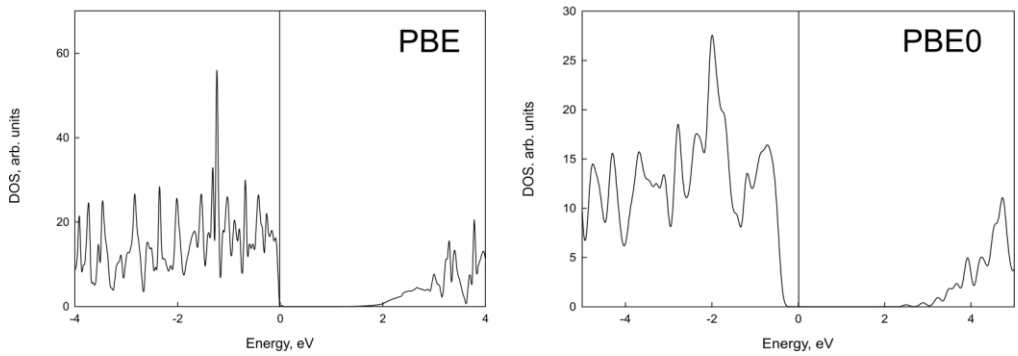

Figure 2. Density of states for β-Bi_2O_3 obtained at PBE and PBE0 level of theory. Energy scale is shifted so the Fermi level is equal to zero.

Table 2. Band gap values for β-Bi_2O_3 and Bi_2SiO_5. Direct/indirect nature of the gap is given in parentheses.

Compound	Band gap, eV			
	PBE	PBE0	B3LYP	HSE06
β-Bi_2O_3	1.31 (indirect M->Γ)	2.47	2.25	1.86
Bi_2SiO_5	2.81 (direct Γ)	4.12	3.93	

3.2 Modeling of β-Bi_2O_3/Bi_2SiO_5 hetero-junction

Structural parameters of β-Bi_2O_3 and Bi_2SiO_5 don't match well so either large supercells or slab rotations are required in order to construct the interface between them. The model interface structure of β-Bi_2O_3 (001) and Bi_2SiO_5 (100)-(√2x√2)R45 surfaces was chosen as it ensures the minimal tension between slabs due to their structural similarities.

Large number of atoms makes it reasonable to perform further calculations using PAO basis which is known to be more efficient for interface structures, as implemented in OpenMX package, instead of the plane waves. Table 1 shows comparison between β-Bi_2O_3 and Bi_2SiO_5 unit cell vectors obtained by the cell optimization performed in both VASP and OpenMX. The latter ones are slightly larger but the difference between two basis sets is less than 1.5% and the results still match the experimental data.

Further calculations of Bi_2SiO_5 and β-Bi_2O_3 surfaces were carried out in OpenMX program package. Figure 3 illustrates hybrid hetero-junction structure obtained during the geometry optimization of the interface.

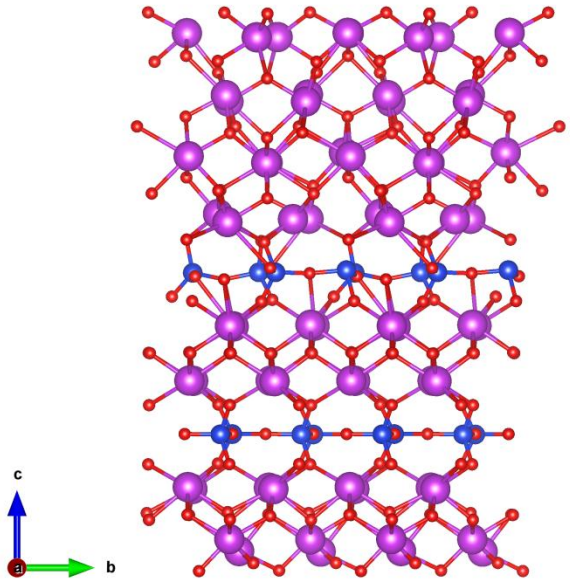

Figure 3. Bi_2SiO_5/β-Bi_2O_3 hetero-junction structure. Bismuth, oxygen and silicon atoms are denoted as purple, red and blue balls, respectively.

Band structure analysis shows significant redistribution of electronic states near the Fermi level comparing to the bulk β-Bi_2O_3 and Bi_2SiO_5 phases (see Figure 4). Hybrid structure possess narrow bandgap of ~0.21 eV while keeping its indirect nature (M->Γ) characteristic for bismuth oxide. Including spin-orbit coupling (SOC) doesn't change the band gap width and character, though there is some visible splitting.

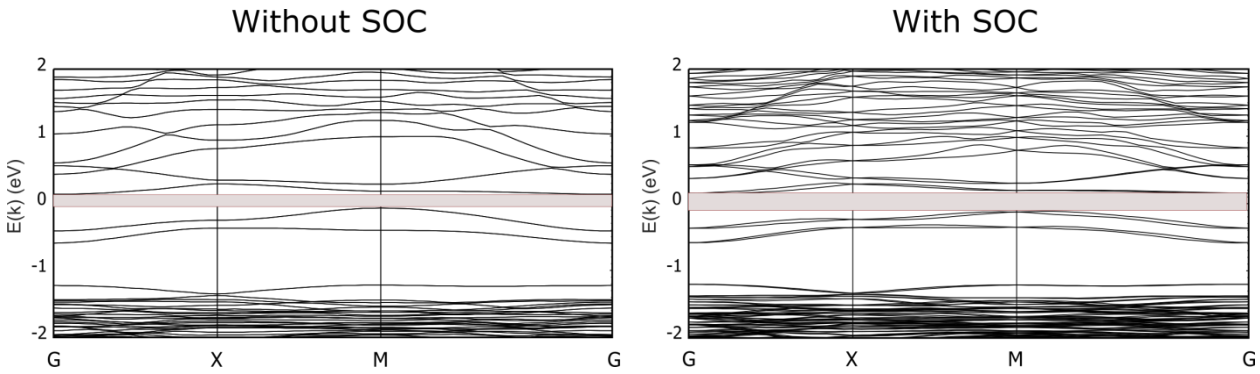

Figure 4. Band structure for Bi_2SiO_5/β-Bi_2O_3 hetro-junction with and without spin-orbit coupling taken into account. Band gap is defined by darker rectangle.

Further analysis of electronic structure reveals that this drastic change should be mainly attributed to Bi_2SiO_5 slab as it demonstrates features completely different from its bulk counterpart (see DOS in Figure 5). New states are emerging in the band gap making the slab metallic in contrast to semiconducting bulk phase. Behavior like that can be associated with the thickness of the model slab which isn't large enough to reproduce the results for bulk as β-Bi_2O_3 slab does. This, however, is not to be concerned about as the present work is aimed to simulate the formation of Bi_2SiO_5 on the β-Bi_2O_3 substrate so using thin film is even preferable and there is no use to overcomplicate the model by adding more layers of Bi_2SiO_5.

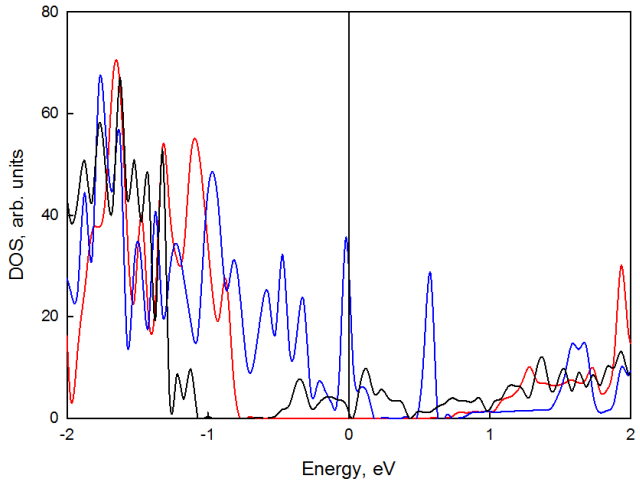

Figure 5. Density of states for β-Bi_2O_3 (001) (red line), Bi_2SiO_5 (100) - (√2x√2)R45 (blue line) slabs and the interface between them (black line).

4. CONCLUSION

Atomic and electronic structure of hybrid β-Bi_2O_3/Bi_2SiO_5 structure has been investigated. Properties of reference bulk compounds were found to be in good agreement with available data. The interface preserves indirect band gap which is characteristic for bismuth oxide. However, the band gap width of hetero-junction is much smaller. Including SOC doesn't change the band structure drastically. Bi_2SiO_5 slab demonstrates emerging of states in the band gap.

ACKNOWLEDGEMENTS

This work was supported by RSF, grant no. 19-73-30026. Authors would like to thank Information Technology Centre, Novosibirsk State University for providing access to their supercomputers.

REFERENCES

[1] He, R., Xu, D., Cheng, B., Yu, J. and Ho, W., "Review on nanoscale Bi-based photocatalysts," Nanoscale Horiz. 3, 464-504 (2018).

[2] Vodyankin, A. A., Ushakov, I. P., Belik, Yu. A. and Vodyankina, O. V., "Synthesis and photocatalytic properties of materials based on bismuth silicates," Kinet. Catal. 58(5), 593-600 (2017).

[3] Duan, J., Liu, Y., Pan, X., Zhang, Y., Yu, J., Nakajim, K. and Taniguchi, H., "High photodegradation efficiency of Rhodamine B catalyzed by bismuth silicate nanoparticles," Catalysis Communications 39, 65–69 (2013).

[4] Hou, D., Hu, X., Wen, Y., Shan, B., Hu, P., Xiong, X., Qiao, Y. and Huang, Y., "Electrospun sillenite $Bi_{12}MO_{20}$ (M = Ti, Ge, Si) nanofibers: general synthesis, band structure, and photocatalytic activity," Phys. Chem. Chem. Phys. 15, 20698 (2013).

[5] Isik, M., Surucu, G., Gencer, A. and Gasanly, N. M., "Electronic, optical and thermodynamic characteristics of $Bi_{12}SiO_{20}$ sillenite: First principle calculations," Materials Chemistry and Physics 267, 124711 (2021).

[6] Li, X., Zhang, W., Li, J., Jiang, G., Zhou, Y., Lee, S. and Dong, F., "Transformation pathway and toxic intermediates inhibition of photocatalytic NO removal on designed Bi metal@defective $Bi_2O_2SiO_3$," Applied Catalysis B: Environmental 241, 187–195 (2019).

[7] Gu, W., Teng, F., Liu, Z., Liu, Z., Yang, J. and Teng, Y., "Synthesis and photocatalytic properties of Bi_2SiO_5 and $Bi_{12}SiO_{20}$," Journal of Photochemistry and Photobiology A: Chemistry 353, 395–400 (2018).

[8] Noh, T. H., Hwang, S. W., Kim, J. U., Yu, H. K., Seo, H., Ahn, B., Kim, D. W. and Cho, I. S., "Optical properties and visible light-induced photocatalytic activity of bismuth sillenites ($Bi_{12}XO_{20}$, X = Si, Ge, Ti)," Ceramics International 43, 12102–12108 (2017).

[9] Li, Q.-Y. and Zhao, Z.-Y., "Interfacial properties of α/β-Bi_2O_3 homo-junction from first-principles calculations," Physics Letters A 379, 2766–2771 (2015).

[10] Perdew, J. P., Chevary, J. A., Vosko, S. H., Jackson, K. A., Pederson, M. R., Singh, D. J. and Fiolhais, C., "Atoms, molecules, solids, and surfaces: Applications of the generalized gradient approximation for exchange and correlation," Phys. Rev. B. 46(11), 6671–6687 (1992).

[11] Perdew, J. P., Chevary, J. A., Vosko, S. H., Jackson, K. A., Pederson, M. R., Singh, D. J. and Fiolhais, C., "Erratum: Atoms, molecules, solids, and surfaces: Applications of the generalized gradient approximation for exchange and correlation," Phys. Rev. B. 48(7), 4978–4978 (1993).

[12] Blöchl, P. E., "Projector augmented-wave method," Phys. Rev. B. 50(24), 17953–17979 (1994).

[13] Kresse, G. and Joubert, D., "From ultrasoft pseudopotentials to the projector augmented-wave method," Phys. Rev. B. 59(3), 1758–1775 (1999).

[14] Kresse, G. and Hafner, J., "*Ab initio* molecular-dynamics simulation of the liquid-metal–amorphous-semiconductor transition in germanium," Phys. Rev. B. 49(20), 14251–14269 (1994).

[15] Kresse, G. and Hafner, J., "*Ab initio* molecular dynamics for liquid metals," Phys. Rev. B. 47(1), 558–561 (1993).

[16] Kresse, G. and Furthmüller, J., "Efficiency of ab-initio total energy calculations for metals and semiconductors using a plane-wave basis set," Comput. Mater. Sci. 6(1), 15-50 (1996).

[17] Kresse, G. and Furthmüller, J., "Efficient iterative schemes for *ab initio* total-energy calculations using a plane-wave basis set," Phys. Rev. B. 54(16), 11169–11186 (1996).

[18] Monkhorst, H. J. and Pack, J. D., "Special points for Brillouin-zone integrations," Phys. Rev. B. 13(12), 5188–5192 (1976).

[19] Morrison, I., Bylander, D. M., Kleinman, L., "Nonlocal Hermitian norm-conserving Vanderbilt pseudopotential," Phys. Rev. B. 47(11), 6728–6731 (1993).

[20] Grimme, S., Antony, J., Ehrlich, S. and Krieg, H., "A consistent and accurate ab initio parametrization of density functional dispersion correction (DFT-D) for the 94 elements H-Pu," J. Chem. Phys. 132(15), 154104 (2010).

[21] Blower, S. K., Greaves, C., "The structure of β-Bi_2O_3 from powder neutron diffraction data," Acta Cryst. C44, 587-589 (1988).

[22] Ketterer, J., Kramer, V., "Crystal structure of the bismuth silicate Bi_2SiO_5," Neues Jahrbuch fur Mineralogie 1, 13-18 (1986).